Numerical Methods in Civil Engineering

A Review on Factors affecting Seismic Pile Response Analysis: A Parametric Study

M. Zarrin[*], B. Asgarian[**], R. Fulad[***]

ARTICLE INFO

Article history:
Received:
May 2017
Revised:
September 2017
Accepted:
October 2017

Keywords:
Soil Pile Structure Interaction, Centrifuge Experiment, Pile Supported Structure, Liquefaction, OpenSees

Abstract:

The seismic soil-pile-superstructure interaction (SSPSI) is one of the most important sources of nonlinear dynamic response of any pile supported structure such as jacket type offshore platforms (JTOP). In recent years, some researchers have studied experimental and real cases of JTOP response under earthquake or cyclic loading using OpenSees software. Throughout a parametric study, the main goal of this paper is to provide designers of pile supported structures supplemental insight into the amount of importance of different parameters included in the SSPSI response. To this end, a beam on nonlinear Winkler foundation numerical model of a single pile embedded in layers of soft clay and dense sand tested in a geotechnical centrifuge was created using OpenSees. The created numerical model was able to successfully capture the response in elastic and intermediate range of nonlinear response. However, the rate of excess pore pressure generation in the model was observed to be faster than the real test results in highly nonlinear events. Subsequently, the sensitivity of the analyzed response to soil shear strength and stiffness parameters was evaluated. The response sensitivity to various input parameters used for definition of pressure sensitive material constitutive behavior - especially the influence of parameters on pore pressure generation – was also investigated. The effects of degradation of p-y behavior after liquefaction on ARS of superstructure and moment distribution of pile were investigated. Moreover, a sensitivity analysis has been carried out to explore the systematic effects of various parameters of clay soil layer on dynamic pile analysis results.

1. Introduction

Evaluating Seismic Soil-Pile-Superstructure Interaction (SSPSI) plays a paramount role in the pile supported structures design procedures, particularly in soft clays and dense sand. A wide range of researches has been devoted to this issue, leading to various approaches with varying complexity and efficiency. The level of complexity required to be considered depends on the purpose of analysis, importance and type of structure, the types of loading that will be experienced in design life, the severity of loading and as a result, the level of nonlinearity in materials. By ignoring the shear transfer between adjacent layers, and accepting Winkler's fundamental assumption (1876) that each layer of soil responds independently to the surrounding layers, an approach named p-y method emerged. In this method, the Beam on Nonlinear Winkler foundation (BNWF) system is discretized to parallel springs trying to represent real soil behavior, and linear beam-column elements connected to these springs. The considerable shortcoming of this method is the two dimensional simplification of the analysis, with no additional efforts for carefully modeling the radial and the slipping mechanism between pile and soil. However, the BNWF method is a versatile and economic method that

** Corresponding Author: Msc. in Marine Structures, Civil Engineering Department, K.N.Toosi University of Technology, Tehran, Iran, PhD candidate, Email:* mo_zarrin@yahoo.com
** Professor, Civil Engineering Department, K.N.Toosi University of Technology, Tehran, Iran.
***PhD candidate, Department of Civil Engineering, University of Central Florida, Florida, USA.

could be applied to take into consideration the various complicated conditions in a simplified manner, which makes it attractive to the engineers. The force displacement behavior of springs has been back calculated from the results of well instrumented pile lateral load tests in different soil conditions (Matlock 1970[34], O'Neill and Murchison 1983[37], API RP 2A-WSD 2000 [2]).

In this paper, the BNWF finite-element model of a pile with a mass as a superstructure on top of it embedded in layers of soft clay and dense sand and tested in the geotechnical centrifuge at the University of California at Davis, was created using OpenSees software. OpenSees (Mazzoni et al. 2007[35]) is an open-source, object oriented software framework for simulating the seismic response of structural and geotechnical systems. In recent years, some researchers have studied experimental and real cases of JTOP response under earthquake or cyclic loading using OpenSees (Zarrin and Asgarian, 2013[60]; Elsayed et al. (2014)[22]; Asgarian et al. 2018[8]). Honarvar et al. (2007)[28] numerically modeled a small-scaled planar prototype platform using OpenSees to evaluate the local and global behavior of pile–leg interaction in JTOPs. Their model lacked soil-pile interaction part. In order to account for tearing and element disconnection of joints, fatigue material was used. Through comparison with test results, it was demonstrated that their analytical model was able to capture the inelastic cyclic behavior of the planar frame of JTOPs as accurately as possible. Asgarian et al. (2008)[6] conducted Incremental Dynamic Analysis of a designed and installed offshore platform in the Persian Gulf with OpenSees, considering Pile-Soil interaction and post-buckling behavior of lateral load resisting elements. They used the same p-y element, which will be evaluated in this paper. Elsayed et al. (2014)[22] presented an approach for the reliability assessment of a fixed offshore platform against earthquake collapse. The results of pushover analysis showed that the platform collapse was identified by multiple failures of the bracing and leg members of the jacket combined with bending failure of piles below mud line. Sharifian et al. (2015)[42] investigated the effects of pile foundation nonlinearity and its influence on the ultimate strength of fixed platforms under seismic loading. They concluded that the pile foundation plays an important role in the dynamic response of off shore platforms, and can drastically alter the ultimate seismic capacity of the platform together with its failure mode. Abyani et al. (2017)[1] investigated the assumption of lognormal distribution of the drift demand and spectral acceleration capacity for the JTOP under earthquake loads. The considered SSPSI in their study was capable of affecting the drift demand distribution. Furthermore, Zarrin et al. (2018)[59] reported that throughout the response of the investigated case study JTOP under some earthquake records at high intensity levels, foundation overturning failure mode could increase the drift demands in jacket story levels. Bea (1991)[12] performed a series of static push-over analyses on a fixed offshore platform, and found that the first nine nonlinear events were concentrated in the foundation piles. As a conclusion, if the factors contributing in the modeling of SSPSI problems are evaluated together with other structural material and element database evaluated in the literature, the whole JTOP problem subjected to earthquake loading can be predicted reliably. This study tends to review a wide range of phenomena related to SSPSI problems, and brings together all the related aspects in a comparative manner. In addition, throughout a parametric study, the aim is to provide supplemental insights into the amount of importance of different parameters included in the SSPSI response for pile supported structure designers. Since shallow layers of soil in the Persian Gulf typically consist of soft clay or loose sand underlain by stiff soils, the results of a centrifuge test that consists of a soft clay layer on top of a dense sand layer was chosen to be compared with the results of the numerical model.

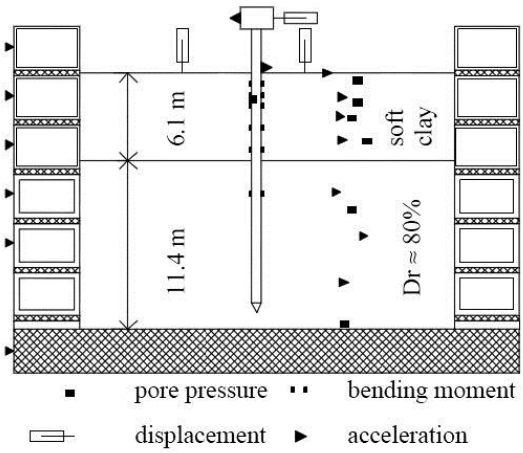

Fig. 1: Schematic of Layout and Instrumentation in tests Csp4 and Csp5

2. Centrifuge Test Data

In the present paper, the simulated finite element model results are compared with the results of centrifuge experiments (Wilson 1998[53]) performed using the large servohydraulic shaking table mounted on the national 9-m radius geotechnical centrifuge at the University of California at Davis (Kutter et al. 1994[32]). The Flexible Shear Beam (FSB) container used for these tests consists of six hollow aluminum rings separated by 12 mm thick layers of soft rubber allowing the container to deform with the soil. All tests were performed at a centrifugal acceleration of 30g. All dimension of results presented herein is in prototype unit. The soil profile consisted of two horizontal soil layers: a very soft clay layer overlaid on a dense sand layer. The sand layer was fine, uniformly graded Nevada sand with C_u= 1.5 kPa and D_{50}= 0.15 mm, at a dry density of 1.66 Mg/m^3. The clay layer was normally consolidated reconstituted Bay mud (LL=88, PI=48) placed in four equal layers, with each layer pre-consolidated under an applied vertical stress. Water was used as pore fluid and saturation was verified with P-wave velocities measured from top to bottom of the soil profile near the container center. A schematic representation of FSB container, soil profile, instrumentation and structural model are illustrated in Fig. 1.

In Centrifuge tests Csp4 and Csp5, two single supported structures and four pile group systems were shaken. In this

paper, pile Sp1 which consisted of a super structure mass of 49.1 ton attached to a single pile embedded in soil profile described earlier has been analyzed. The pile had been driven into soil profile before spinning. The pile material was aluminum with a flexural stiffness of 417 MN.m^2, which is equivalent to a 0.67-m-diameter steel pipe pile with a 19 mm wall thickness.

The considered tests in this study are Csp4 and Csp5 test series, each shaken with several simulated earthquake events with the peak ground accelerations ranging from 0.055 g to 0.7 g and from 0.035 g to 0.6 g, respectively. Each of these events was a scaled record of Port Iland in 1995 Hyogoken-Nambu Kobe (Csp-4) and Santa Cruz in the 1989 Loma Prieta earthquakes (Csp-5), which were filtered before the analyses. Detailed description of the soil profile, structural properties, earthquake event details, and results of centrifuge experiment can be found in (Wilson 1998[53], Boulanger et al. 1999[15], Wilson et al. 1997a[51] and 1997b[52], Asgarian et al. 2013[7]).

3. Adopted soil properties for dynamic response analysis

In this section, fundamental properties of the soil material, which are essential to perform free filed site response analysis for computing input ground motions to the BNWF model will be explained. In the present research, the undrained shear strength C_u profile of the upper clay soil layer before centrifuge spinning was calculated from the below relationship (Boulanger et al. 1999):

$$C_u=0.35\ \sigma'_{vc}\ OCR^{0.8} \quad (1)$$

where σ'_{vc} = effective vertical consolidation stress, OCR = the over consolidation ratio (OCR= $\sigma'_p/\ \sigma'_{vc}$), and σ'_p= vertical preconsolidation stress. As proposed by Boulanger et al (1999), for all the analyses herein, a unique C_u profile which is the average of after and before shaking C_u profiles plus a 15 percent increase was adopted.

Hardin and Drnevich (1970)[26] showed that shear modulus values of cohesionless soils are strongly influenced by the confining pressure, the strain amplitude, and the void ratio (equivalently relative density). However, they are not dependent on the variations in grain size characteristics or other factors. Thus, due to this finding, a simple equation (which relates the confining pressure and relative density to shear modulus) proposed by Seed and Idriss (1970)[40] has been used throughout this research in order to calculate low strain shear modulus of the lower sand layer:

$$G= 219K_{2,max}\sqrt{\sigma'm} \quad (2)$$

Where $\sigma'_m= (1+2K_0)\sigma'_{vc}/3$; and K_0=0.6. According to Seed and Idriss (1970)[40], for sands with relative density of about 80%, $K_{2,max}$ = 65. In this equation the effect of relative density and strain can be expressed through their influence on soil modulus coefficient, $K_{2,max}$. For modulus reduction curve (G/G_{max}), the upper range G/G_{max} versus shear strain relationships for sand proposed by Seed and Idriss (1970)[40] was used. This reduction curve is the default reduction curve of pressure dependent material in OpenSees FE software.

For the clay, by matching the soil profile's fundamental period at very low strain levels, a G_{max}/C_u=380 ratio was proposed for the computation of low strain shear modulus. For this purpose, the adopted C_u profile explained above was used. Since modulus reduction curves play an important role in determining the results of ground response analysis, special care is needed for choosing appropriate reduction curves for clay based on the available literature. The modulus reduction curves reported by Vucetic and dorby (1991)[48] for normally and over consolidated clays with plasticity index of 50 are appropriate for higher clay layer of centrifuge model. The shear modulus reduction curve corresponding to 10 cycles – to account for the effect of cyclic stiffness degradation on G/G_{max} – for plasticity index of 50 recommended by Vucetic and dorby (1991)[48] was used. The G/G_{max} at large strains was modified to limit the peak shear stress to the seismic C_u value [i.e., $\tau_{peak}= C_{u,cyc}=G\Upsilon_{peak}$, giving $G/G_{max}= C_{u,cyc}/(G_{max}\Upsilon_{peak})= C_{u,cyc}/(380Cu\Upsilon_{peak})$].

4. Free field soil response

The first step in any uncoupled SSPSI analysis is computation of soil profile horizontal response as a function of depth to vertically propagating shear waves. In the present report, the soil profile response was computed by taking the advantages of ndMaterial class and solid elements of OpenSees FE software. Commonly for stimulating the saturated soil deposit dynamic response, a two-phase material based on Biot (1962)[14] theory for porous media is used. In OpenSees, four-node plane strain quadUp element implements a simplified numerical formulation of this theory known as U-P formulation, in which the primary unknowns are the displacements of soil skeletons U and pore pressure P (Chan 1988[19]). Herein, a single column of soil composed of 175 quadUp elements each of which has 50 m length, 1 m width and 0.1 m height was modeled in 2D plane. The permeability coefficient of k= 3.1e-5 m/s for sand with Dr = 80% and, k = 1e-9 m/s for clay (Holtz and Kovasc 1981[27]) were used.

In the present model, for stimulating the stress-strain behavior of sand and for Bay mud, the PressureDependentMultiyield (PDMY) material and the PressureIndependentMultiYield (PIMY) material of OpenSees material database were used, respectively. In different depths of sand layer, the reference mean effective confining pressure (σ'_{mr}) values were defined according to the values used for computation of shear modulus of soil based on the Seed and Idriss (1970)[40] relation. In the absence of detailed laboratory data, other parameters required for definition of these materials were defined according to the recommended values of developers of materials for medium-dense sand with relative density of 65%-85%, which is available in OpenSees Command Language manual (Mazzoni et al. 2007[35]). Since the hollow rings encompass the soil, each side of the soil has the same displacement as the other side. For stimulating this behavior, the periodic boundary condition was assumed to mimic a 1D analysis behavior.

The dynamic analysis was performed in two stages: firstly, performing the gravity analysis step assuming that

the soil material behaves linearly elastic. Secondly, after completion of the gravity step, the material condition was changed to elastic-plastic condition prior to application of seismic loads. Approximate Minimum Degree – AMD – (Amestoy et al. 2004[3]) numberer was used to determine how degrees of freedom are numbered. This numberer object solved convergence problems during gravity analysis step in our model with fine meshes, and also led to faster convergence in dynamic analysis.

5. Uncoupled Dynamic SSPSI Analysis

A BNWF numerical model was created in the finite element program OpenSees to perform uncoupled seismic SSPSI analysis. For the modeling of pile elements in OpenSees, nonlinear beam column element was utilized. The pile consists of a number of Force-Based Beam Column (FBBC) elements (De Souza 2000[21]) each of which is 0.2 m long in upper clay layer, and 1 m long in underlying dense sand layer. The number of elements in above soil surface part was four. Zero length elements whose force-deformation constitutive behavior represents soil near field springs are connected to every node of pile below the soil surface. Uniaxial p-y, and t-z (skin friction) and q-z (end bearing) material objects in the lateral and vertical directions, respectively, were assigned to these zero length elements.

5.1 Nonlinear p-y elements

Soil lateral spring nonlinear behavior was modeled using the Pysimple1 uniaxial material (and its liquefaction based counterpart material "PyLiq1") incorporated in OpenSees by Boulanger et al. (2003)[16]. The constitutive rules for this spring and for non-liquefaction are described in Boulanger et al. (1999)[15] except for minor changes described in Boulanger et al (2003)[16]. The nonlinear p-y behavior is conceptualized as consisting of Elastic ($p\text{-}y^e$), Plastic ($p\text{-}y^p$) and Gap ($p\text{-}y^g$) components in series. A radiation damping dashpot is placed in parallel with elastic element. The gap component itself is composed of a nonlinear closure spring ($p^c\text{-}y^g$) in parallel with a nonlinear drag spring ($p^c\text{-}y^g$).

The constitutive behavior of the Pysimple1 material for clay was based upon Matlock's relations for soft clay[34] under static loading condition. API RP2A-WSD (2000)[2] recommended p-y backbone relation for drained sand is approximated by Pysimple1 material for modeling of cohesion less soil. Boulanger et al. (1999)[15], and Assareh and Asgarian (2008)[10] showed that the resulting p-y curves based on the formulation of Pysimple1 material for both clay and sand soils match with API p-y curves within a few percent over the entire range of y.

In the current study, the input parameters P_{ult} and y_{50} for upper bay mud layer which are the ultimate capacity of p-y material and the displacement at which 50% of P_{ult} is mobilized during monotonic loading, were computed based upon Matlock's (1970)[34] equation. C_u was taken based on the adopted C_u profile described in the previous sections. During the cyclic lateral loading, gaps develop in cohesive soils. When the pile is moving within these gaps in subsequent cycles, the water inside the gaps exerts a drag force on the sides of the pile. This residual resistance is accounted for in Pysimple1 material formulation through a parameter C_d, defined as the ratio of the residual resistance to the ultimate resistance P_{ult}. This parameter was assumed to be 0.3 for clay according to back-calculated p-y curves obtained from these centrifuge experiments (Wilson 1998[53]). The inclusion of gaps change the shape of compression and tension p-y curves from vertical S-shape to horizontal " ~ " shape.

Properties of p-y springs for dense sand layer were calculated based on API recommendation for sand, which do not include the effects of liquefaction. The friction angle was taken as 38 degrees similar to the one adopted for free-field analysis. As stated before, the backbone of p-y curve for drained sand condition was based on hyperbolic curve presented in API. Herein, the same equation was used to calculate the value of y_{50} needed for the definition of Pysimple1 material but with modifications in terms of the increase in stiffness with depth and the effect of soil layering condition. The values of modulus of subgrade reaction (K) in API formula are commonly taken from a recommended curve in API. These values for k are based on drained lateral load tests that are dominated by soil behavior at low depth. Thus, at a depth of more than a few pile diameters, it has been known to overestimate the initial stiffness (Es) of P-y springs. Also, a modification for effective overburden pressure effects was used for computing the modulus of subgrade reaction as follows (Boulanger et al. 2003[16]):

$$K^* = C_\sigma K \quad , \quad C_\sigma = \sqrt{\frac{\sigma_{ref'}}{\sigma_{v'}}} \tag{3}$$

Where K*= corrected modulus of subgrade reaction; $\sigma_{ref'}$ = reference stress at which k was calibrated, taken as 50 kPa. The effect of soil layering was taken into account by an approach proposed by Georgiadis (1983)[24]. In this method, the p-y curves for upper soil layer are calculated according to the standard criteria for homogenous soils. For the lower layer, P_{ult} values are determined assuming that an upper layer of soil has the same material as layer below it, and by finding the equivalent depth of this hypothetical layer.

The parameter C_d was given 0.1 in definition of the Pysimple1 material for lower sand layer. As stated before, C_d is the ratio of residual strength to ultimate resistance of p-y spring. The results of previous back-calculated p-y behavior for liquefying sand from laboratory tests and FEM analysis (Wilson et al. 2000[54]), generally showed that p-y characteristic is consistent with the known stress strain response of liquefying sand. This means that the typical cyclic p-y curve has a contraction phase, a phase transformation part which leads to large permanent deformations and a hardening part, which is due to dilation tendency of cohesionless soils. This is similar to inverted S-shaped p-y characteristics of cohesive soils. From the observed p-y curves (Wilson et al. 2000[54]), the chosen value of C_d seems reasonable.

In Pysimple1 constitutive equation, radiation damping is modeled by a dashpot on the far-field elastic ($p\text{-}y^e$) components in series with gap component and nonlinear hysteretic component. Herein, the dashpot coefficient is determined based on the recommendation of Wang et al.

(1998)[49], which is a modification of work done by Berger (1977)[13].

In the analysis presented in the following sections, the "PyLiq1" material model was used instead of Pysimple1 material. The constitutive characteristic of this material is the same as PySimple1 material with modification for the effects of free field excess pore pressure in the adjacent soil element. A key parameter in this material is "pRes" which is the residual subgrade reaction that the material retains when the adjacent solid soil elements have zero effective confining stress (r_u = 1). In all analysis presented in the following sections, the pRes value was set about 0.1 of initial ultimate capacity of soil. This value is a common assumption which was proposed by Liu and Dobry (1995)[33] for Dr = 40 & 60 % and have also been used in Boulanger et al. (2003)[16] and some other studies. The effects of this parameter on response will be investigated in detail in section 8.

6. Simulation Results

The different earthquake events of CSP4 and CSP5 were exerted on the model, and the recorded experimental results and the analyzed responses are given in the following figures. The recorded results of the centrifuge tests are available in detail in University of California at Davis website[47]. A comparison between the calculated and experimentally recorded peak superstructure acceleration in various events is shown in Fig. 2(a) (See reference model results). In general, the created model in OpenSees tended to underestimate the structural responses. On average, the numerical results were 36 % smaller than test results in Csp4 and 3 % smaller in Csp5. The Csp5 calculated results showed excellent agreement with the test results. Since, the superstructure displacements and pile bending moments appeared to be correlated to superstructure accelerations, they weren't presented here. Analyzed and recorded acceleration response spectra (ARS) for the superstructure during events B-E in Csp4 is plotted in Fig. 2(b) (See reference model results). The under estimation trend is also noticeable in this figure. From the test results, it can be inferred that the equivalent "fundamental" period of the whole soil-pile-structure system changed from 1 second in low shaking level to 1.95 second in high shaking level. This was the consequence of occurrence of nonlinearity in the soil profile, especially in the clay layer. The created numerical model was able to successfully capture this trend in elastic (eventCsp4-C) and intermediate (events Csp4-B and to a lesser extent event, Csp4-D) range of nonlinear response, but the frequency content of the motion of superstructure changed in analyzed events Csp4-D and Csp4-E. Furthermore, the discrepancy between the amplitude of spectral acceleration in the numerical model and tested model became significant in event Csp4-D and Csp4-E. The possible reason for this behavior was that the rate of excess pore pressure generation in the model was faster than the real test results, which led to higher values of r_u (r_u = excess pore pressure to effective vertical stress ratio) in sand layer whereas r_u lay under 0.5 in Csp4-D and 0.85 in Csp4-E recorded results at depth 9.6 m. The softened soil caused the peak spectral period of structure to be shifted from 1.95 s to 2.1 s, in event Csp4-E. The time history of r_u is depicted in Fig. 3 during events Csp4-D and Csp4-E.

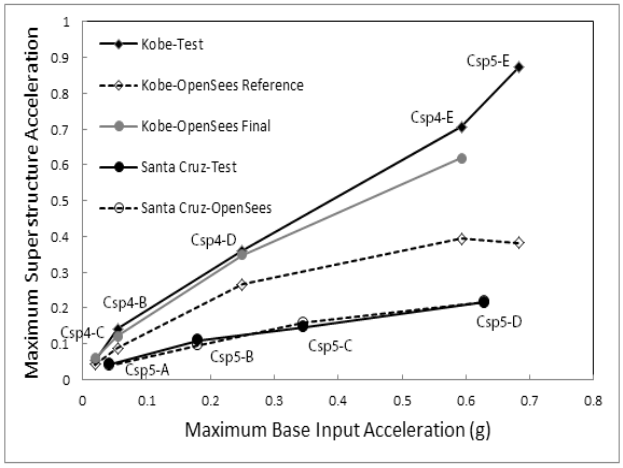

a) Peak Superstructure Acceleration

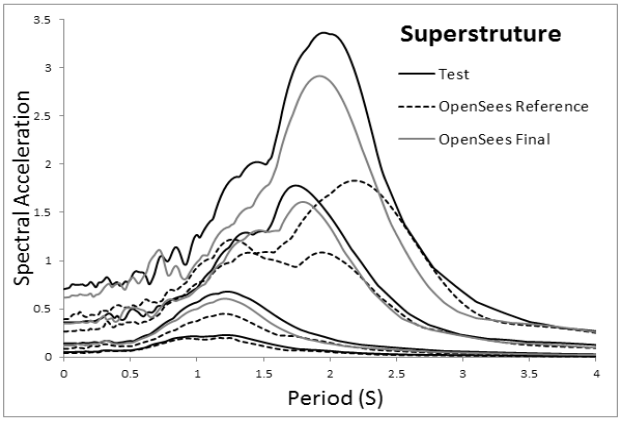

b) Superstructure ARS (5% damping)

Fig. 2: Analyzed and Recorded results during Events Csp4 and Csp5 for SP1

Herein, two different earthquake records (Kobe and Santa Cruz) were chosen for comparison purposes to evaluate the sensitivity of model response to frequency content of different motions. As is seen in Fig. 2(a), the results of analyzed model agreed fairly well with recorded peak motions for all levels of intensities in Csp5 events showing that the integrity of estimated model results highly depends on frequency content of motions. The reason that numerical model responded less strongly to Csp5 tests was that the Santa Cruz input motion had smaller spectral accelerations in the 1 s to 2 s period range than did the Kobe input motion (Boulanger et al. 1999[15]).

7. Improved set of input model parameters in sand layer

The simulated results of OpenSees model created based on the parameters chosen according to the available experimental data were presented in the preceding section. The input parameters for the definition of materials and elements were attempted to be chosen as carefully as possible based on common previous research works. The results showed that the model had some shortcomings in the highly nonlinear range of response according to recorded centrifuge data. The possible sources of this bias could be classified as inappropriate chosen properties of soil such as

shear strength and stiffness parameters, the disability of utilized material and elements in predicting real response, inappropriate input parameters used for definition of PDMY and PIMY constitutive behavior and some other factors such as the effects of soil-container interaction, influence of the pile foundations on the soil profile motions, limitations in the signal processing, and scale effects. In this section, the sensitivity of analyzed response to first three sources will be evaluated by changing the constitutive soil strength properties and also using different input parameters of PDMY material. The focus will be placed on parameters mostly affecting the fluid solid fully coupled interaction response, especially the influence of parameters on pore pressure generation.

A procedure is available to choose the parameters that control liquefaction potential of PDMY based on Cyclic Resistance Ratio (CRR) of soil. The capacity of the soil to resist liquefaction is expressed in terms of cyclic resistance ratio (CRR), referred to as liquefaction resistance or liquefaction resistance ratio. This ratio is commonly determined using the liquefaction potential curves, for example refer to the report on liquefaction proposed in NCEER (1997)[58]. In this procedure, a single element with the properties of cohesionless soil under investigation is constructed. Thereafter, it is subjected to uniform, stress-controlled cyclic shear stress loading obtained from associated CRR value, which should result in liquefaction in 15 cycles. This procedure was used by Boulanger et al. (2003)[16], Cooke (2000)[20] and Byrne et al (2004)[18] to numerically model liquefied soils. However, since liquefaction potential curves are valid for $(N_1)_{60}$ SPT values of less than 30 and CPT values of less than 150, which approximately corresponds to a sand with relative density of 65 -70 % (NCEER 1997[58]), it is not applicable to our case of interest with Dr = 80 %. Alternatively, 8 different models were constructed with manually adjusting the soil parameters, which will be discussed in detail in the following sub sections.

7.1 Stress densification effects

Cohesionless soils are routinely placed in uniform density through air pluviation method in centrifuge models under 1g acceleration condition and, then, spun up to higher acceleration fields causing non-uniform stresses in soil profile with higher stresses at surface and lower stresses at base. These increased stresses induce compaction in the soil which leads to higher and non-uniform density of the model (Byrne et al. 2004[18], Park and Byrne 2004[38]). The amount of densification has been estimated from one-dimensional compression tests at the laboratory and has been found to be dependent on initial density and square root of vertical effective confinement. Park and Byrne (2004)[38] through examination of compression data on a number of sands, proposed an equation in terms of initial placement density and subsequent applied vertical stress. Herein, according to their relationship and maximum, minimum and placement dry density of dense sand which are available in Wilson (1998), the updated relative density was computed 77.3% at the top of sand layer and 79.2 % at the base of model. The average deviation (2.7 %) in density of sand from its initial value (75.7 %) indicates that stress densification is not a source of concern in the present paper.

7.2 Degree of saturation effects

Initial degree of saturation is seen to be very important and can have a significant effect on pore pressure build-up. The pore fluid pressure change is related to the change in volume of pore fluid using its bulk stiffness or bulk modulus. When soil is fully saturated, the pore fluid phase consists of only water and the bulk modulus of pore fluid is equal to bulk modulus of water, i.e. $B_f = 2.2 * 10^6$ kPa. The solution of air in water gives the effect that the soil is compressible. Dissolved air in water significantly affects the bulk stiffness of air-water mixture. The inclusion of even 1 % air in the soil is sufficient to significantly reduce the pore fluid bulk modulus to $1* 10^4$ kPa (Fredlund and Rahardjo 1993[25]). Any change in fluid bulk modulus directly affects the displacement of model and pore pressure generation during loading (Yang 2000[55]).

To clarify the effect of saturation, in model 1, the same material and parameters as the one used for reference model were utilized except a reduction in bulk modulus of fluid to a value of $2.2*10^5$ kPa. This reduced B_f value approximately corresponds to a 99.8 % degree of saturation. Fig. 3 shows that the generated excess pore pressure decreased from state of $r_u = 1$ in the reference model to values with the excellent matches with test results in Csp4-E event. The acceleration response of soil calculated at depth 8.3 m (Fig. 4) also shows excellent improvement relative to reference model. From Fig. 5, it's observed that ARS of superstructure was improved both in amplitude and peak period. However, the generated excess pore pressure and consequently, acceleration and ARS of superstructure in event Csp4-D didn't change significantly. These results show that reducing B_f could have noticeable effects in response but can't improve results in all amplitudes. Fortunately, in the current centrifuge tests the P-wave measurements were recorded to be 1000 m/s or greater; therefore, the degree of saturation was expected to be 99.9% or higher (Balakrishnan 2000[11] and Wilson 1998). However, due to the fact that the model could not be fully saturated, in the following models, a slightly reduced weighted value ($B_f/n = 1.25*10^6$ kPa) was used. This value is close to $B_f/n = 2.2*10^6$ kPa, which was used during the calibration process of PDMY material (Yang 2000[55]).

7.3 Contraction parameter effects

Previous liquefaction studies have introduced the concept of phase transformation (PT) surface in stress-space. Within the PT surface during undrained loading or outside of it during unloading phase, contraction always take place resulting in increased pore pressure and decreased effective confinement (Yang et al. 2003[57]). In PDMY material constitutive model, the contractive (inside PT surface), perfectly plastic (on PT surface), and dilative (outside PT surface) phases of response were taken into consideration by formulating a non-associative flow rule in each phase. Herein, to investigate the effect of the parameter that

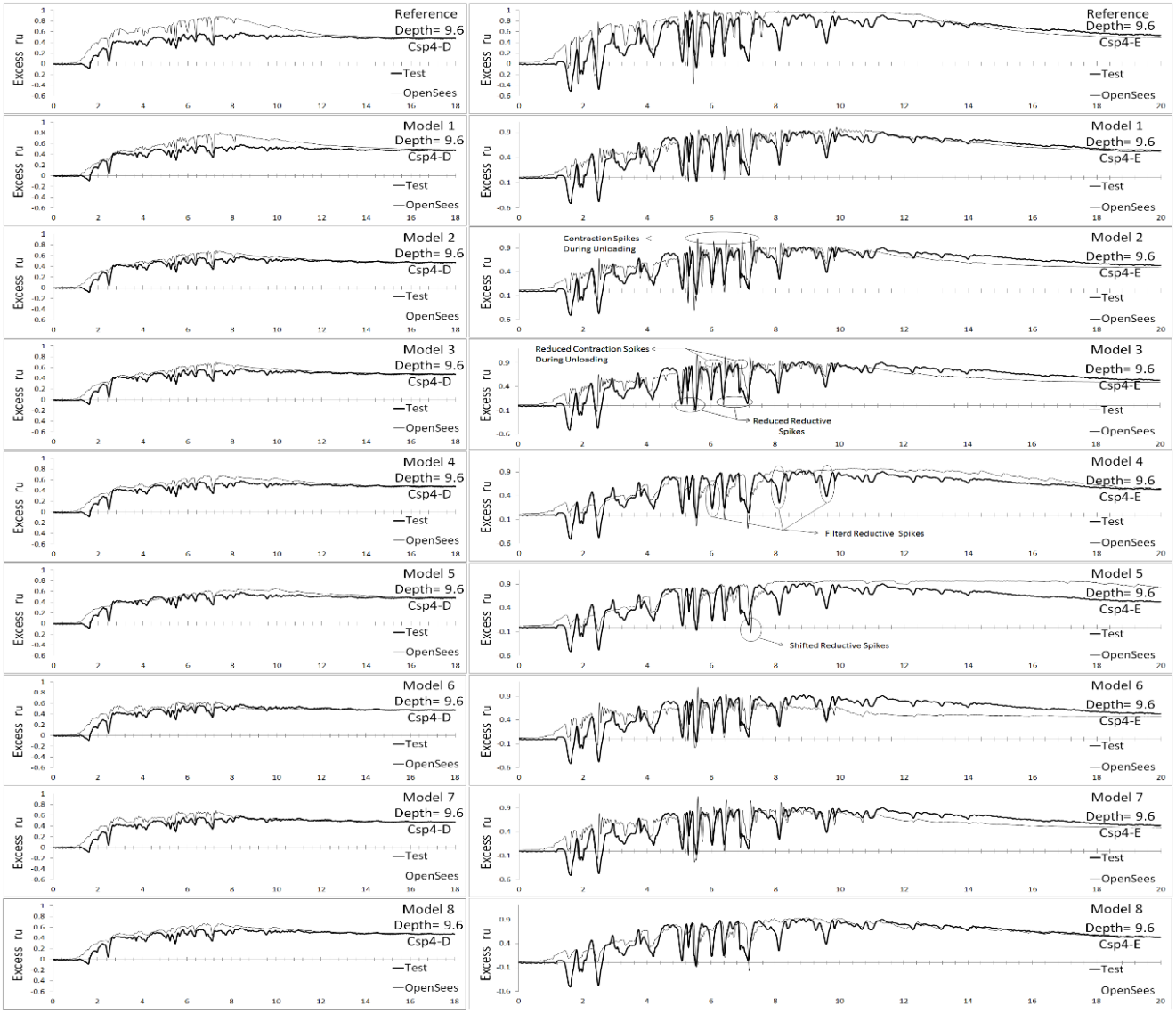

Fig. 3: Excess r_u time history for various models during events Csp4-D and Csp4-E.

controls the flow of strain during contraction and consequently, generation of excess pore pressure, a model with different contraction parameter was created. In model 2, the same material and parameters as the one used for reference model were utilized except a reduction in contract1 parameter of material definition from 0.05 to 0.03. Contraction1 defines the rate of shear-induced volume decrease (contraction) or pore pressure buildup. This parameter is the main key in controlling the pore pressure generation potential of PDMY material while the sensitivity analysis showed that other parameters have less effect on the pore pressure buildup. As it can be seen from Fig. 3, the generated pore pressures in this model reasonably agree with the recorded data in event Csp4-E. In spite of displaying some discrepancies, in event Csp4-D, the generated excess pore pressures have been improved relative to both reference and model 1. Consequently, ARS of superstructure in Csp4-D and Csp4-E events were improved comparatively to reference model. These results show that reducing parameter that defines the rate of shear-induced volume decrease has more performance in adjusting r_u values with test results in various CSRs than reducing bulk modulus of fluid to imaginary values.

7.4 Dilation parameter effects

Medium to dense cohesionless soils firstly compress, when subjected to lateral shear loading (Section 7.3). But at larger strains, as the soil grains roll over one another, they regain their stiffness, which in turn raises a tendency to dilate. This volume increase results in a decrease in pore water pressure and increasing effective stress. As a consequence, associated instances of pore-pressure reduction and acceleration spikes are observed in excess pore pressure time history and lateral acceleration time history, respectively. Such dilation tendency and acceleration spikes have been observed in many of the laboratory tests, shake table tests, In-situ seismic response and centrifuge tests such as the one studied here. In PDMY material constitutive model, this sharp dilation tendency is activated when the stress state goes above PT surface. A specific flow rule has been formulated for this behavior,.

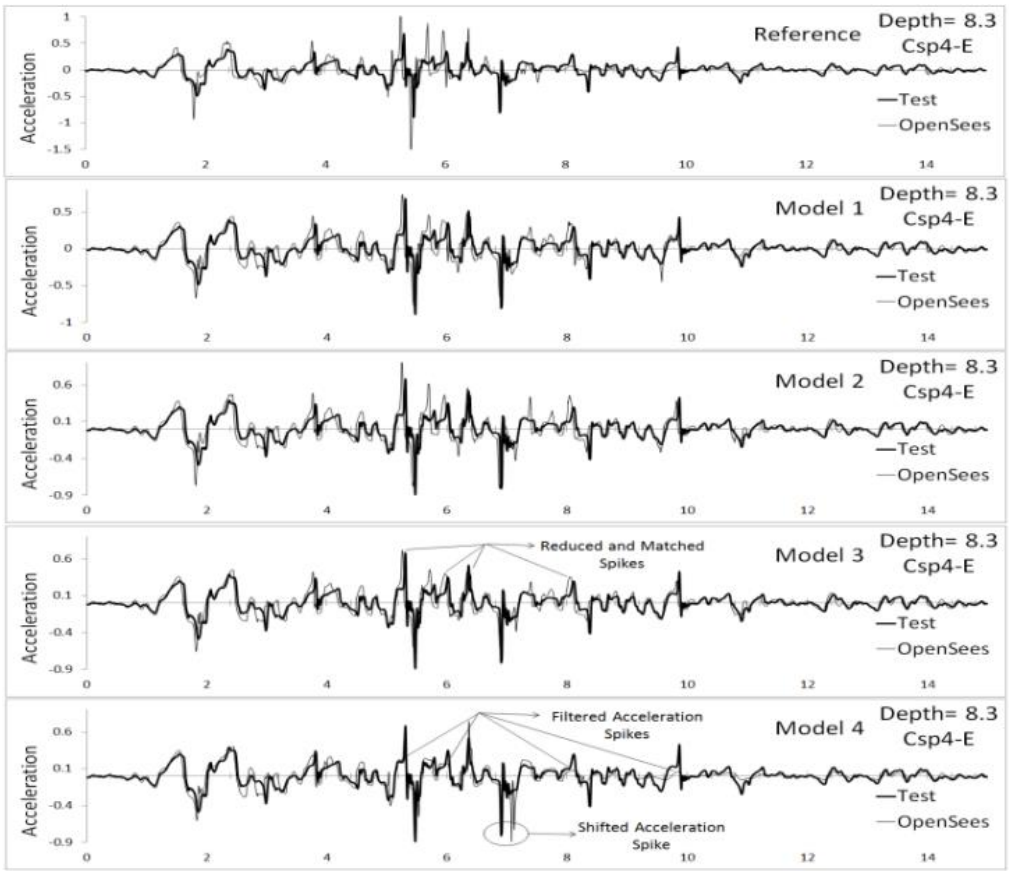

Fig. 4: Acceleration time history of soil in various models

which depends on two material constants, dilation1 and dilation2 parameter where larger values correspond to stronger dilation rate. One of the specifications of this flow rule is that the dilation tendency progressively increases with cumulative octahedral plastic strain generated during current dilative phase (Yang et al. 2003[57]). In model 3, the same material and parameters as the one used for model 2 were utilized except a reduction in dilat1 parameter of material definition from 0.6 to 0.4. Firstly, we discuss the observed spikes in the previous models. It should be noted that no acceleration spikes were observed in event Csp4-D due to the fact that spikes occur around the onset of liquefaction (r_u = 1) (Yang 2000[55]). In Csp4-E event in reference model, acceleration and reductive excess pore pressure spikes (see Figs. 3-4) were larger in magnitude than the test results, mainly because of the occurrence of liquefaction (very low effective confinement).

In model 1, both acceleration and reductive excess pore pressure spikes surprisingly equaled to test results indicating that, whenever the excess pore pressure history becomes equal to recorded value, the acceleration history becomes close to true value. In model 2, while the excess pore pressure history was consistent with recorded result, the spikes were larger in magnitude. By reducing the dilat1 parameter in model 3, the spikes became consistent with test results without any other major change in excess pore pressure and acceleration history showing that dilat1 is a parameter to control the magnitude of spikes in the model. It is noteworthy that sensitivity analysis showed that dilat2 parameter has a very low effect on calculated response.

Based on experimental observation, the rate of contraction during unloading is dictated to a significant extent by preceding dilation phase (eg. Nemat-Nasser and Tobita 1982[36]). In PDMY material constitutive model, a distinctive flow rule has been defined for unloading phase, which implicitly relates the rate of contraction to the extent of accumulated confinement during dilation phase (Yang et al. 2003[57]). From Fig. 3, it is observed that in all models, after the dilation phase (Excess pore pressure reductive spikes) and during unloading above PT surface (contraction), the magnitudes of r_u exceeded the measured results. This shows that the model could not efficiently predict the rate of contraction during unloading. However, by comparing model 3 and 2, it can be concluded that by reducing dilat1 parameter the amount of this deviation decreases implying that the rate of contraction depends on preceding dilation phase in the models. It is believed that this deficiency has a negligible effect on acceleration response (see Fig. 4) and superstructure response (see Fig. 5).

7.5 The influence of previous dilation history

In model 4, PDMY02 material was used instead of PDMY Material. A major modification made in this material is the addition of a parameter to account for the influence of previous dilation history on subsequent contraction phase. The flow rule developed for contraction phase of response in this material is dependent on two material constants. The first parameter is similar to that of PDMY material, and the second parameter takes into consideration the effect of

plastic volumetric strain accumulated during dilation phase on current contraction rate of response (Yang et al. 2003[57]). Sensitivity analysis showed that using the default value of this parameter led to better results while changing it made the fluctuation of excess pore pressure unreal. In model 4, parameters of PDMY02 material were chosen according to recommended values for sand with Dr = 75% in OpenSees command language manual. From Fig. 3, it is observed that in Csp4-D event the model generated reasonable excess pore pressure similar to previous models. In Csp4-E event, the calculated response showed general agreement with measured results until time 9 second but beyond this time, the rate of excess pore pressure dissipation was lower than recorded values. Changes to other parameters of PDMY02 material had no influence on the improvement of this inconsistency. Comparing results of model 3 and 4 revealed that in this material, instances of pore pressure increase during subsequent unloading was filtered due to utilization of contrac2 parameter. Looking deep into Figs. 3-4 indicates that this material filters some reductive spikes in r_u, and consequently, some acceleration spikes along with a shift in time of occurrence of some of the spikes whereas these deficiencies didn't occur in PDMY material results. However, these inconsistencies are less important from the ARS of superstructure point of view as the ARS of superstructure in event Csp4-E in model 2 and 4 were the same (wasn't shown in Fig. 5).

7.6 Soil shear stiffness effects

Arulnathan et al. (2000)[5] presented a method for measuring in-flight shear wave velocity of Nevada sand in Centrifuge models. Their proposed relationship for estimation of shear wave velocity in Nevada sand with Dr = 80% was:

$$V_s = 0.136 V_{pw} \left(\frac{\sigma'_m}{P_a} \right)^{0.25} \quad (4)$$

where V_{pw} (= 1550 m/s) is the *p*-wave velocity of water and P_a is the atmospheric pressure in the same units as σ'_m. Using this empirical relationship for computation of G_{max} in sand resulted in values which are 46% lower than the G_{max} values computed based on Seed and Idriss (1970)[40] relation. In model 6, the input G_{max} values in soil profile were determined according to this empirical relationship. Other parameters for material definition were the same as model 4. In general, the computed Excess r_u time history in this model is similar to that of model 4 with some higher values after 8 seconds (Fig. 3). Even after reducing contrac1 parameter (eg: using 0.009 instead of 0.013) no improvement occurred to this inconsistency after 8 s. In addition, some phase lag was observed in r_u reductive spikes. These phase lags are also noticeable in acceleration history of soil (not shown in Fig. 4) showing that computing soil shear stiffness based on Arulnathan et al. (2000)[5] relationship makes the basic features of model inconsistent. The computed equivalent fundamental period of superstructure in event Csp4-E was lengthened relative to other cases perhaps due to the fact that higher r_u values (mainly after 8 s) caused the soil to liquefy in vicinity of interface of two layers of soil. Furthermore, the softened soil shear stiffness possibly contributes to this lengthening.

7.7 Effects of change in permeability (Constant increased permeability)

Previous experimental studies have emphasized on the influence of permeability on liquefaction potential and associated deformations of cohesionless soils. It is now obvious that a soil with lower permeability can cause faster pore pressure generation and slower dissipation of excess pore pressure, and as a result more susceptibility to liquefaction state. Spatial variation of permeability in a soil profile is also of special concern specially, when a liquefied soil layer is overlaid by a relatively impermeable layer. In this case, due to the hydraulic gradient, a thin trapped layer of water would form beneath the impermeable layer, and speed up pore pressure buildup in this region leading to unexpected liquefaction (Yang and Elgamal 2002[56]). Moreover, the permeability of soil is the main key in settlement of soil profile since the dissipation and drainage of pore pressure are highly dependent on the amount of permeability. The dissipation of pore pressure takes place either during early seconds of seismic shaking where the rate of pore pressure build-up is higher than dissipation rate, or after the end of seismic excitation (Ishihara 1994[31]). Thus, the appropriate value of permeability could promote the simulated accuracy of excess pore pressure and settlement prediction if the soil constitutive model has the capability of taking into consideration the amount of settlements. On the other hand, even choosing a proper value of at rest permeability is unlikely to lead to an accurate prediction of excess pore pressure history since investigations have shown that rate of water flow increases during the liquefaction period, mainly due to disruption of soil structure (Ishihara 1994[31], Shahir et al. 2012[41]). The increased rate of water flow is interpreted as increase in the permeability coefficient of soil.

Commonly, a practical way for taking into consideration the change of permeability during liquefaction process is using "Constant increased permeability". Different increase factors have been used by previous researchers ranging from a small value of 4 times the initial value (Taiebat et al. 2007[44]) up to 10 times the initial value (Balakrishnan 2000[11]). In model 6, to investigate the influence of permeability on soil and superstructure response, permeability of dense sand layer was increased by a factor of 4. The other parameters of sand material were defined similar to the reference model. According to Fig. 3, the generated excess pore pressures in event Csp4-D reduced comparing to other models and became closer to experimental values. On the contrary, the r_u values in event Csp4-E reduced significantly compared to other models in all times and became lower than test results. These indicate that increasing the permeability would accelerate the dissipation of excess pore pressure in all stages of response. Reduced r_u values lead to smaller acceleration spikes relative to models with higher r_u values. In this model, both the amplitude and equivalent period of superstructure (see Fig. 5) became closer to measured values proving the importance

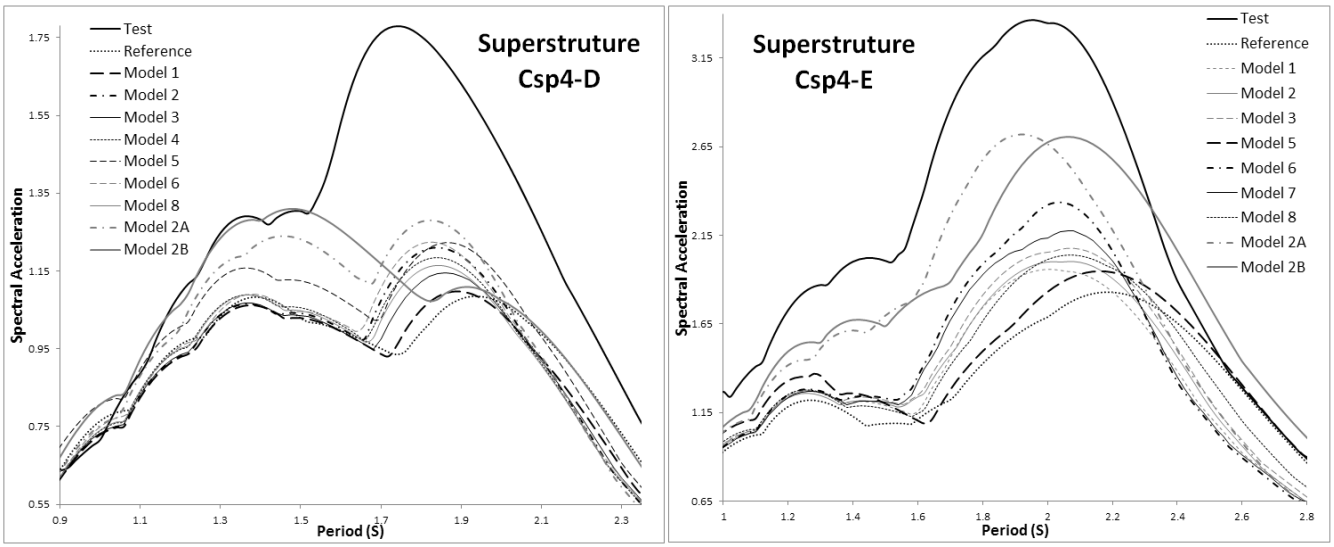

Fig. 5: ARS of superstructure during events Csp4-D and Csp4-E for various models

of excess pore pressure prediction and magnitude of acceleration spikes on soil pile structure interaction.

7.8 Effects of variation of permeability

Shahir et al. (2012)[41] by comparison of numerical simulation results and the centrifuge experiment measurements indicated that there is a direct relationship between the permeability coefficient and excess pore pressure ratio during build-up, liquefaction and dissipation phases. Therefore, a simple power function was proposed to describe variation of permeability during seismically induced liquefaction. Their proposed relationship was in the following form:

$$k_b/k_i = 1+(\alpha-1)*r_u^{\beta} \qquad (r_u \le 1) \qquad (5)$$

Where k_b is the soil permeability coefficient during seismic shaking, k_i is initial (at-rest) permeability coefficient before shaking and α and β are positive material constants. This equation shows a gradual increase of permeability with the rate defined by β up to the onset of liquefaction when the permeability becomes equal to α times of the initial permeability (r_u = 1), and also a gradual reduction in permeability once more with the rate defined by β in dissipation phase of response.

Table 1. different calibrated β parameters for build-up (b) and dissipation (d) phases

	$r_{u(b)}<0.7$	$0.7<r_{u(b)}<1$	$0.7<r_{u(d)}<1$	$r_{u(d)}<0.7$
Model 7	0.5	2	12	12
Model 8	4	4	7	9

In model 7 and 8, a code has been written in OpenSees main domain which obtains the pore pressure response using OpenSees miscellaneous commands in every time steps of analysis and in all elements along soil column and computes the inflight r_u values. Subsequently, using the above equation the updated permeability coefficients are computed in all elements and the permeability values of quadUp elements are changed using update Parameter command in Opensees. In model 7, the PDMY material was used whereas, in model 8, the PDMY02 material was used. The sensitivity analysis resulted in the calibrated α parameter equal to 4 and 3 for model 7 and 8, respectively. In these models different β parameters were calibrated for build-up and dissipation phases as shown in table 1. Fig. 3 reveals that the pore pressure time history in model 7 was improved corresponding to reference model, and was also very close to model 2 results. Fig. 5 also shows that calculated ARS of superstructure was improved relative to model 2 which can be interpreted as a slightly lower r_u history in comparison with model 2. From Fig. 3, it can be concluded that the variable permeability in model 8 resulted in improved r_u history after time 9 sec comparatively to model 2, without producing any significant changes in ARS of superstructure.

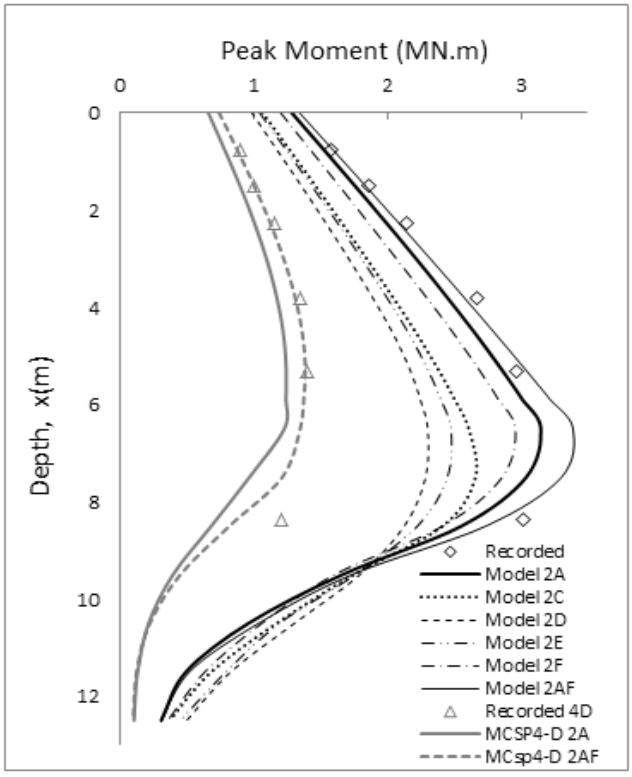

Fig. 6: Maximum bending profile along depth in various models

Table 2. Peak superstructure acceleration response deviations in different models relative to test results

	Record (g)	Refrnc M %	M 1 %	M 2 %	M 3 %	M 4 %	M 5 %	M 6 %	M 7 %	M 8 %	M 2A %	M 2AF %
Csp4-C	0.052	-19.74	-19.70	-19.72	-19.72	-19.74	-12.60	-19.70	-19.73	-19.74	-19.72	13.56
Csp4-B	0.141	-38.31	-38.54	-38.52	-38.52	-38.49	-30.74	-38.48	-38.48	-38.49	-38.34	-14.69
Csp4-D	0.360	-26.18	-25.70	-26.19	-26.15	-25.56	-19.77	-25.15	-25.26	-25.54	-13.02	-3.37
Csp4-E	0.706	-44.21	-41.38	-41.74	-37.76	-35.38	-38.45	-38.76	-40.50	-37.85	-15.82	-12.35

These results show that using a variable permeability instead of a fixed permeability is another issue in enhancing the accuracy of predicted responses. However, it doesn't introduce additional improvement in calculated responses relative to change in contraction parameter of PDMY and PDMY02 materials and perhaps, it is still easier to adjust the responses with contraction parameters. The reason might be attributed to the fact that PDMY and PDMY02 materials have been calibrated with the assumption of constant permeability (Yang 2000[55] and Yang et al. 2003[57]).

Peak superstructure acceleration response deviations in different models compared to test results are given in table 2. What can be inferred from this table is that all 8 predicted model responses have been improved respective to reference model in highly nonlinear range (event Csp4-E). However, the predicted responses in average sense in all models in Csp4-E are 38 % smaller than the test results.

8. Parametric study on dynamic P-Y behavior in sand

In this section, the effects of degradation of p-y behavior after liquefaction (r_u of 1 as one definition of liquefaction) on acceleration response spectra of superstructure and moment distribution along depth of pile are investigated. Several centrifugal experiments (Liu and Dobry 1995[33], Wilson 1998), large shake table tests (Tokimatsu et al. 2001[45], Tokimatsu and Suzuki 2004[46]) and full scale blast induced liquefaction tests (Weaver et al. 2005[50] and Rollins et al. 2005[39]) have reported fundamental aspects of subgrade reaction behavior between piles and liquefied soils. These studies revealed that the observed dynamic p-y behavior for liquefying sand in different ranges of density is consistent with the known stress-strain response of liquefying sand. The back calculated p-y behavior after liquefaction in loose sand show very little or negligible lateral resistance against pile, even under large relative displacement. In medium dense sand, both the stiffness and strength of p-y behavior degrades as the prior relative displacement, the number of cycles and pore pressure ratio increase. Furthermore, the p-y behavior has been observed to be displacement hardening as the relative displacement approached or exceeded maximum past values, and as the strains between soil and pile is large enough to move the sand through the phase transformation.

Very few tests have presented the results of back calculation of p-y curve in dense sand. Based on a work by Tokimatsu et al. (2001)[45] in dense sand, p-y curves in some aspects have characteristics similar to that of medium dense sand such as concave upward shape of p-y curves and dependency on prior relative displacement. However, besides this study, Tokimatsu and Suzuki also (2004)[46] showed that subgrade reaction doesn't degrade even after liquefaction (ru =1) in dense sands. On the other hand, Boulanger et al. (2003)[16] used a ratio of S/σ'vc (S is Residual strength of liquefied soil) equal to 0.1 in dense sand layer to reduce the ultimate strength of dense sand in fully liquefied condition, which corresponded to a reduction multiplier (mp) of 0.43 when ru is 0.6. Brandenberg (2005)[17] used an even lower value (mp = 0.3) for his study. Although these studies were for pseudo-static pushover analysis of lateral spreading cases, however, the peak bending moment occurred in the transient part of bending time history. This inconsistency is also true for potential evaluation of triggering of liquefaction in dense sands. While conventional liquefaction potential curves (NCEER 1997[58]) suggest that liquefaction don't occur in dense sands, two recent centrifuge experiments (Zeng and Liu 2012[61], and Ganainy et al. 2012[23]) on very dense sands revealed that this type of sand experiences full liquefaction. Observation in high excess pore pressure, de-amplification in acceleration records and ground surface settlement of soil confirm this. However, Ganainy et al. 2012[23] test results showed that full liquefaction was only restricted to shallow depths of about 1 m. Moreover, Sze and Yang (2014)[43] presents a systematic experimental investigation into the impact of specimen preparation on the cyclic loading behavior of saturated sand. They reported that dense sand exhibited the cyclic-mobility pattern no matter which reconstitution method was used. However, the flow-failure type response did not occur in dense sand. With these differences in the reported results in mind, in this section the influence of various methods proposed in the literature for taking into account the degradation of p-y behavior after liquefaction on the moment response of pile will be explored.

"PyLiq1" material model in OpneSees domain is implemented by Boulanger et al. (2003)[16] to simulate the afro-mentioned conditions of liquefaction on p-y behavior (refer to section 5). The initial ultimate capacity of material during analysis is scaled linearly (Liu and Dobry 1995[33]) by a factor of $(1-r_u)$ with this limitation that the capacity can't be smaller than pRes. Furthermore, the stiffness (coefficient of subgrade reaction) of p-y curves is also scaled with this linear reduction factor. Imamura (2010)[30] performed a series of centrifuge model tests to investigate the characteristics of horizontal subgrade reaction of piles in liquefiable sand and proposed a two-constant parameter relation based on r_u value which is more or less similar to linear relation between r_u and coefficient of subgrade

relation (Figure 8 in Imamura 2010[30]). The closure spring in PyLiq1 constitutive model could simulate the influence of prior relative displacement on p-y behavior. Weaver et al. (2005)[50] performed some analysis with just reducing the ultimate strength of p-y curves and neglecting changes in coefficient of subgrade reaction and effects of prior relative displacement. By comparing analyses results with the results of measured full scale blast induced liquefaction, they concluded that moment distribution in simplified analysis methods differ significantly from that of measured values.

All of the above mentioned advantages of PyLiq1 suggest that this material is capable of simulating the key characteristics of liquefied p-y behavior. One of the deficiencies of this material is the dependency of response on only far field r_u value, while now it is evident that the induced pile strain has some effects on near field excess pore pressure (Rollins et al. 2005[39]). Tokimatsu et al. (2001)[45] studied this phenomenon in detail and showed that regardless of whether pile or soil displacement dominates the relative displacement, always a compression and extension stress state develops on both sides of the pile. On the compression side r_u is always near to one and reduction of r_u because of combined effects of near field and far field dilation on extension side provide resistance to relative movement between soil and pile. This reduction in pore pressure is always more significant than far field values perhaps due to drainage of water in opened gaps between soil and pile (Weaver et al. 2005[50]), and straining of the soil because of pile movement. However, it is believed that the near field values are closely related to the far field values (Wilson 1998).

There are two general ways to compute pRes value in PyLiq1 material in order to consider the degradation of subgrade reaction during liquefaction. The first approach is to apply reductive scaling factors, or p-multipliers (mp), to the p-y resistances. Ashford et al. (2011)[9] summarized the published recommendations of some researchers for p-multipliers in one single figure. As it was stated before, the recommended values differ significantly with each other for dense sand. An alternative to the p-multiplier method is to compute pRes based on soft clay p-y models, where the residual strength of the liquefied soil is used in place of the undrained shear strength of the soft clay. Several procedures have been proposed for determining residual strength of the liquefied soil, but all produce highly uncertain estimates of residual strength. What complicates their use is the fact that all of these procedures have been proposed based on back-calculation from observed flow slide case histories of sands with SPT corrected blow counts less than 15 and then extrapolating them to higher SPT values. Residual strength of sands have been presented in two manners, one directly relates SPT values to residual strength and the other one expresses it in the form of a normalized residual strength, i.e., a ratio of residual strength to initial effective overburden pressure (S/σ'_{vc}).

In all the analysis performed in the previous sections, the pRes value was set at about 0.1 of initial ultimate capacity of soil, which according to current practice seems a reasonable value (refer to section 5). In order to determine the influence of this parameter on model response, in model 2A, all the parameters were set similar to model 2 except using PySimple1 material instead of Pyliq1 material. Fig. 5 reaction due to liquefaction, the simulated response became closer to recorded response which is in good agreement with Tokimatsu et al. (2001)[45] and Tokimatsu and Suzuki (2004)[46] findings and recommendation of Architectural Institute of Japan (AIJ) (refer to Ashford et al. 2011[9]). However, in this case the fundamental period of the whole system was a little bit smaller than the recorded value, which means that the model is stiffer than the real case suggesting that the p-y curves should be scaled down slightly. In order to emphasize on the importance of this section parametric study, in model 2B, the parameters were once more assigned ~~a~~similar to that of reference model except using PySimple1 material instead of Pyliq1 material. Fig. 5 clarifies that the simulated fundamental period is remarkably longer than the recorded results implying the necessity of predicting true excess pore pressure in sand layer. Moreover, in this case the pattern of calculated maximum bending moment in larger depths differed significantly from the recorded results. In model 2C, the p-multiplier of model 2 in previous section was increased to a value of 0.45 based on the recommendation of Brandenberg (2005)[17]. Fig. 6 shows the maximum bending moment distribution along depth in event Csp4-E for new models created in this section. As it can be seen in this figure, model 2A shows a reasonable agreement with recorded results. On the other hand, model 2C predicted the moments less than measured values in all depths. However, the depth corresponding to peak bending moment in this model is slightly deeper than model 2A, which agrees more with the actual results.

As it was mentioned earlier, another way to induce liquefaction effects on p-y curves is using residual strength of soil. Idriss and Boulanger (2007)[29] proposed a direct relationship between residual strength of soil and SPT corrected blow counts using previous work data. Their relationship suggests absolutely high residual strengths (higher than drained values) for dense sands in our case, which accords with recommendation of Architectural Institute of Japan (AIJ). They proposed two other relationships between normalized residual strength and SPT corrected value. The one which neglects void redistribution effects again leads to high residual strength of soil. The other relationship gives $S/\sigma'_{vc} = 0.5$ for dense sand with Dr = 75 %. In model 2D, this ratio has been used to compute the pRes values along depth. From Fig. 6, we can see that this model remarkably under predicted the maximum bending moment values. The configuration of centrifuge experiment in this paper makes a void redistribution likely to occur beneath the nonliquefied clay layer, but no direct sign of the occurrence of this phenomenon was observed. Anderson et al. (2012)[4] measured in-flight the shear strength of liquefying sands in a seismic geotechnical centrifuge model by pulling thin coupons (plates) horizontally through the soil models. They plotted the results of their measurement in terms of S/σ'_{vc} versus SPT corrected blow counts. Although they didn't establish any relationship, but their data is extrapolated herein to compute the S/σ'_{vc} ratio for dense sand. In model 2E, a $S/\sigma'_{vc} = 0.7$ is used based on Anderson et al. (2012)[4] work. Fig. 6 shows that the results of this model was somewhat between results of model 2C and model 2D.

9. Sensitivity to dynamic Clay layer Parameters

In order to provide a better insight into the effects of various parameters of clay soil layer on dynamic pile analysis results, a sensitivity analysis was carried out. This section tends to investigate which of the parameters included in the analysis plays the most important roles in decreasing the uncertainty of simulation consistency with recorded results. Also, it is intended to explore their relative effects on the various response parameters such as Peak Superstructure Acceleration (PSSA) and bending moment distribution along pile depth. Consequently, instead of increasing and decreasing a single set of specified parameter, a continuous variation of that parameter has been studied in order to find a systematic influence of that parameter on pile response.

Firstly, the Cu profile was changed, resulting in corresponding changes in the site response parameters (Gmax/cu was held constant) and the p_{ult} values for the p-y elements. The cu profile was reduced and increased by 40% with increments of 10%. The analysis results are presented herein in terms of peak soil and superstructure acceleration, peak bending moment in both depths of 0.7 m and 8.4 m in Csp4-E event and 6.5 m in Csp4-D event in order to investigate the change in maximum bending moment along depth of the pile. The depth 8.4 in Csp4-E event was chosen due to the fact that in this depth the calculated bending moment was significantly lower than the recorded values (see Fig. 6). The depth 6.5 in Csp4-D event was also chosen since the maximum bending moment along whole depth happens near this depth. The results are depicted in Fig. 8, where the vertical axis is the deviation of calculated response from the recorded response, and horizontal axis is the variation of studied parameters relative to base case Model 2A parameters. Moreover, Fig. 7 shows peak soil acceleration at depths of 1.65 & 3 & 8.3 m versus C_u/C_{ur}. Fig. 7 reveals that with reduction in Cu in both events, the peak acceleration of clay layer along depth of soil was reduced. This figure also shows progressive de-amplification of soil accelerations as we approach the surface of layer due to the fact that shear stresses exceeded the shear strength of soil in upper portion of clay layer. On the contrary, the acceleration at the top of sand (a lowered value by a factor of 0.4 is shown in Fig. 8 in event Csp4-E) was inversely correlated to change in Cu which means that with softening of clay layer the sand layer vibrates more freely. From Fig. 8(a), the first finding, as it might be expected, is that the peak bending moment at depth 0.7 m is closely related to PSSA in all ranges of Cu.

Both of the events studied herein show that the bending moment in higher portions of pile near soil surface is always dependent on superstructure inertia, and is not related to any other parameter. Furthermore, According to Fig. 8(a) in event Csp4-D, the reduction in Cu led to lower peak superstructure accelerations, which seems to be related to reduction in free field accelerations (less kinematic loads) due to softening of soil (see Fig. 7). In this event since the shaking was not strong enough to drive the soil to its final resistance, the change in PSSA with Cu was more significant than in event Csp4-E. As the Cu was lowered, the maximum bending moment at depth 6.5 m in event Csp4-D and at depth 8.4 in event Csp4-E was increased implying that the depth at the largest bending moment increased as a result of softening of upper soil layer, as would be expected for a pile foundation loaded primarily by the inertia of the superstructure. In addition to inertial forces, it is likely that kinematic forces in larger depths contributed to this increase in bending moment, though the effects were less significant than inertial effects. When looking with careful attention into both Fig. 8(a) and Fig. 7, the pattern of change in peak acceleration at depth 8.3 with Cu was qualitatively consistent with pattern of change in maximum bending moments at depths 6.5 & 8.5 m, proving the former statement.

In contrast to event Csp4-D, with variation in Cu in event Csp4-E no remarkable change was displayed in PSSA despite the fact that the free field soil movements progressively decreased with decreasing Cu. Since this event was strong enough, the calculated soil shear stresses reached the ultimate shear strength of the clay, and no more loads were transmitted to the pile from movement of soil (Ultimate subgrade reaction reached). Furthermore, independency of PSSA from free field movements suggests that the inertial forces from superstructure dominate the response of pile. A reduction tendency in PSSA with increase in C_u in event Csp4-E might be attributed to this fact that the rate of increase in P_{ult} is higher than increase in soil acceleration. The significant decrease in maximum bending moments at larger depths implies that this increased P_{ult} provided much lateral resistance for soil. It is noteworthy that a sudden reduction in PSSA in Cu/Cur = 1.3 was attributed to a sudden reduction in adjacent peak soil acceleration. One another fact that is concluded from Fig. 8(a) is that if the Cu profile is chosen based on precise measured value and a reasonable judgment, the model is capable of predicting the response more closely to real values than any other profile of Cu (note to lower deviation in PSSA in base case).

The deviation in pile response with change in shear modulus reduction curve of soil is depicted in Fig. 8(b). As stated before, the modulus reduction curves for clay presented by different investigators differ significantly from each other. Therefore to investigate its effects on soil and pile response, a sensitivity analysis has been carried out using modulus reduction curves proposed by Vucetic and dorby (1991)[48] for clays with different PI values. The curves included in these analyses covered the probable range of curves proposed for different clay types. Fig. 7 indicates that the soil accelerations progressively increased when using curves with higher PI value. Higher PI curves correspond to stiffer cyclic soil characteristics. Similar to increase in C_u effects, in this case, the soil accelerations on the top of dense sand decreased when using stiffer modulus reduction curves. Fig. 8(b) indicates that when the shear modulus reduction curve became softer, the PSSA in both events diminished due to decreased soil acceleration. On the contrary, making the soil cyclic characteristics stiffer led to some what inconsistent results, which makes the interpretation of results more difficult. Complicating the problem is the fact that stiffening of free field soil without any change in near field p-y behavior makes the studied cases in this figure an imaginary case. The model with PI =200 in event Csp4-E responded in a consistent manner with

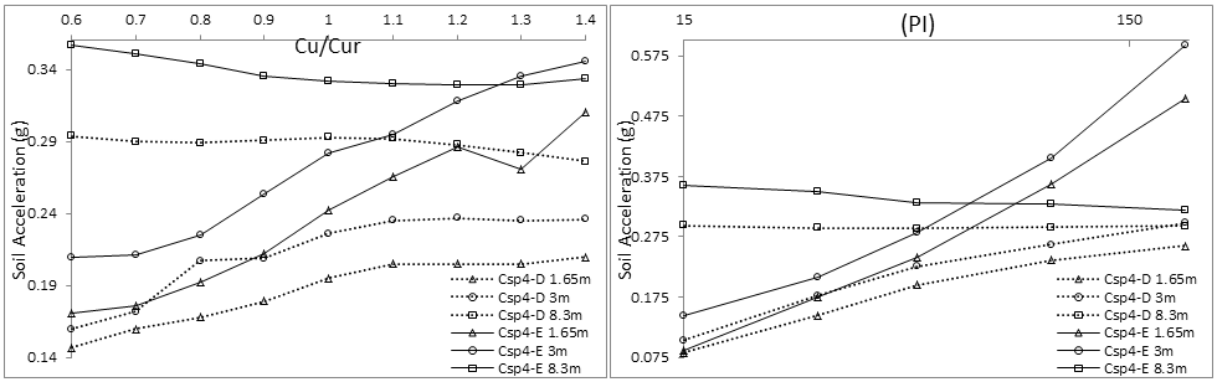

Fig. 7: Peak soil acceleration evolution with change in C_u and shear modulus reduction curve

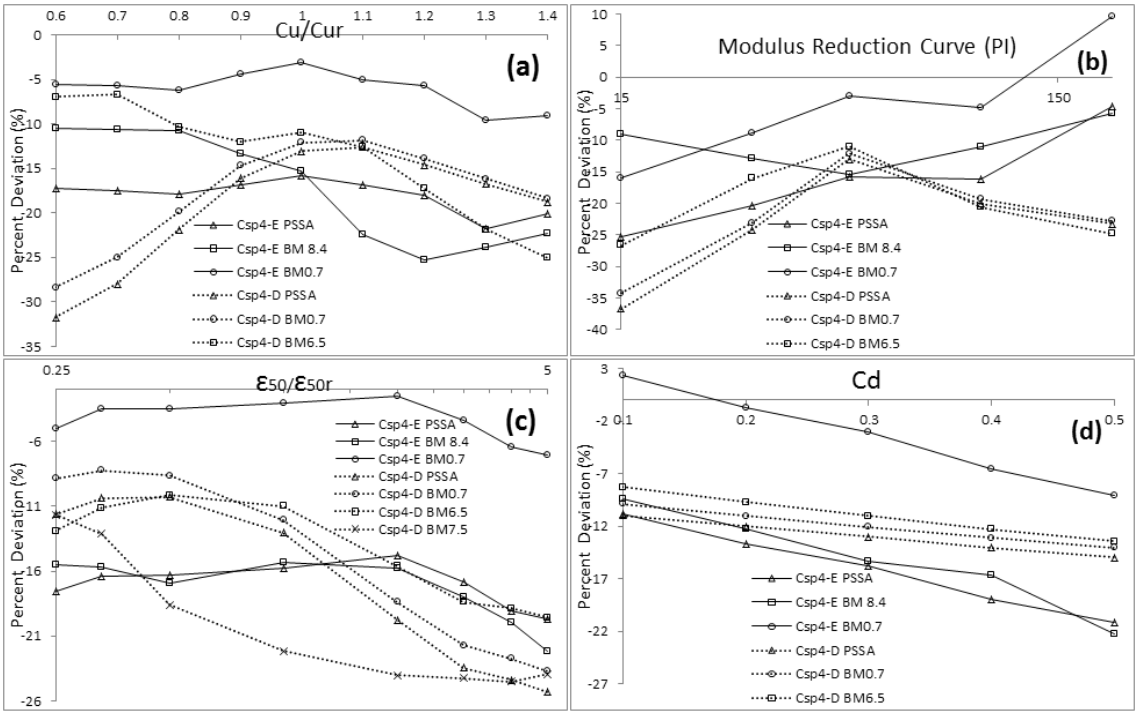

Fig. 8: Evolution in pile response parameters with change in clay layer properties

the soil acceleration increase in this particular case. On the other hand, the model with PI =100 in event Csp4-E showed similar PSSA value as model 2A. The PSSA in model with PI =100 occurred at time 12.47 s, while it was occurred at time 11.52 s in model 2A.

Fig. 8(c) illustrates the relation between deviation in response from recorded results with change in strain corresponding to a stress of 50% of the ultimate stress in a laboratory stress-strain curve (ε_{50}) . This figure -similar to Figs. 8(a),(b) and (d) - also emphasizes on the close relation between PSSA and peak bending moment at shallower depths. In contrast to effects of variation in C_u on calculated response, in this case a systematic correlation between the variation of ε_{50} and how the response was changed could be obtained especially in event Csp4-D. As can be seen from Fig. 8(c), the PSSA was reduced more or less linearly with the increase in ε_{50} in event Csp4-D. Increasing ε_{50} made the p-y curves softer, and this weakened p-y behavior transferred fewer kinematic forces to the pile. As a result the pile vibrated with lower amplitude. Another reason that proves less imparted load to the structure is the direct trend between maximum bending moment in depth 6.5 m and PSSA implying that the bending moment profile along all depths were consistently reduced as a result of reduction in inertial forces (PSSA). A distinct trend between Figs. 8(a)-(c) is that the patterns of variation of PSSA in both figures were the same in event Csp4-D which was attributed to the imparted load to the pile from soil. While in Fig. 8(c) the reduction in transferred load to pile was only attributed to reduced stiffness of p-y curves, in Fig. 8(a) the reduction was because of combined effects of decrease in soil movement and -to a lower extent- reduction in ultimate strength of p-y curves. The reduction in ultimate strength of soil led to increase of maximum bending moment at larger depths. In Fig. 8(c), since the ultimate strength of p-y curves remained constant, the bending moment at larger depths didn't increase, but just reduced as a result of less inertial force. According to Fig. 6, the calculated maximum bending moment at depths larger than 6.5 m in event Csp4-D reduced abruptly, while recorded results showed that up to depth of 8.4 m no sudden reduction in maximum bending moment

happened. Fig. 8(c) shows that reducing ε_{50} progressively improved predicted bending moment at depth 7.5 m. In event Csp4-E, in the ranges of $\varepsilon_{50}/\varepsilon_{50r}$ =0.25 up to 2, the response of pile didn't change remarkably and beyond this value a slight reduction in response was observed, which again was attributed to less imparted load to the pile from soil. This finding implies that the response of pile was only dominated by superstructure inertia and interaction between clay soil and pile played an insignificant role in addressing the response.

Fig. 8(d) illustrates the correlation between changes in residual resistance of p-y curves (Cd) and calculated response parameters. This figure shows a completely linear trend between Cd and all response parameters. With decrease in Cd, less resistance was provided for the pile against its movement in the opened gaps and consequently the pile vibrated with higher amplitude. The reference value of Cd = 0.3 was chosen with qualitative observation of back calculate p-y curves of these centrifuge experiments in Wilson (1998) while careful attention to those back calculated p-y curves shows lower value in some p-y loops. Calculated drag force based on the calculated maximum relative velocity between soil and pile at depth 1.6 m by authors was even lower than ratio 0.1. Especially in larger depths it seems reasonable to use lower Cd values since the P_{ult} values are larger and relative velocity of pile is lower.
According to findings in this section, a final model labeled as model 2AF has been built with modified ε_{50} value to 0.002 and Cd to 0.1. As it is depicted in Figs. 2(a), 2(b) and 6 and table 2 the peak superstructure acceleration, superstructure ARS and maximum bending moments along depths of soil in various events agreed excellently with recorded results

10. Summary and Conclusion

In this paper, a BNWF numerical model of a single pile embedded in layers of soft clay and dense liquefying sand tested in the geotechnical centrifuge was created in OpenSees. In general, the created model tended to underestimate the structural responses in highly nonlinear cases. The sensitivity of analyzed response to soil shear strength and stiffness parameters and to various input parameters used for definition of pressure sensitive material constitutive behavior - especially the influence of parameters on pore pressure generation - was also investigated by creating 8 other models in this paper. Then, the effects of degradation of p-y behavior after liquefaction on acceleration response spectra of superstructure and moment distribution along depth of pile were investigated. A sensitivity analysis has also been carried out to investigate the effects of various parameters of clay soil layer on dynamic pile analysis results. The main findings of the investigations can be summarized as follows:

- It is unlikely that the soil is completely saturated in reality, and initial degree of saturation is seen to have a significant effect on the combined bulk modulus of fluid. Both the combined bulk modulus of fluid and the parameter which defines the rate of shear-induced volume decrease (contraction) or pore pressure buildup have been found to play significant roles in controlling the pore pressure generation potential, while the sensitivity analysis showed that other parameters have less effect on the pore pressure buildup. Results showed that changing the parameter which defines the rate of shear-induced volume decrease has more efficiency in adjusting the r_u values with the test results in various amplitudes than changing bulk modulus of fluid to imaginary values.
- In the model which takes into consideration the influence of previous dilation history on subsequent contraction phase, instances of pore pressure increase during subsequent unloading are filtered in contrast to reference material results. Also, results indicated that this effect filters some reductive spike in r_u. However, the ARS of superstructure in the most severe event, Csp4-E, revealed that the filtered spikes have no effect on structural response.
- Reducing the permeability value caused the r_u values in event Csp4-E to be reduced significantly relative to other models in all time and became lower than test results. These indicate that increasing the permeability would accelerate the dissipation of excess pore pressure in all stages of response and in some cases could lead to biased response.
- Using a variable permeability instead of a fixed permeability is another issue in enhancing the accuracy of predicted responses. However, it doesn't introduce additional improvement in calculated responses relative to the change in the parameter, which defines the rate of shear-induced volume decrease (contraction) of utilized materials. Perhaps, it is still easier to enhance the predicted responses by varying the contraction parameters.
- Contrary to some previous reports, the parametric study in this paper showed that subgrade reaction doesn't degrade even after liquefaction (r_u =1) in dense sands. This finding is in agreement with the findings of some other researchers.
- The change in undrained shear strength and shear modulus reduction curve of clay layer led to somewhat inconsistent results, which were too complicated to be interpreted. However, when the shaking is strong enough to drive the soil to its final resistance, the change in response with variation of these parameters becomes less significant. In the case of changing strain corresponding to a stress of 50% of the ultimate stress in a laboratory stress-strain curve (ε_{50}) and drag force ratio in the opened gap (C_d), a systematic correlation between variation of these parameters and how the response was changed has been observed.
- In all of the sensitivity analysis to dynamic clay layer parameters, the fundamental period of the whole system remained unchanged while the period changed as a result of variation in sand layer properties. This implies that in soil profiles similar to this study case, the period of the system is governed by the underlain stiffer soil.

The results obtained from this study emphasize the capability of numerical models in predicting reliable responses in terms of intensity and frequency content only if the input parameters are selected based on accurate measurement and adequate insight into their effects on response.

References

[1] Abyani, M., Asgarian, B. and Zarrin M. (2017) "Statistical assessment of seismic fragility curves for steel jacket platforms considering global dynamic instability", *Ships and Offshore Structures*, **13**(4):366-374.

[2] American Petroleum Institute, (2000), *"*Recommended practice for planning, design and constructing fixed offshore platforms - working stress design*", API recommended practice 2A-WSD, 21st Ed*.

[3] Amestoy, P., Davis, T. A. and Duff, I. S. (2004)", Algorithm 837: AMD, An approximate minimum degree ordering algorithm", *ACM Transactions on Mathematical Software*, **30**(3), 381-388.

[4] Anderson, I., Hargy, J., Alba, P. and Dewoolkar, M. (2012), "Measurement of residual strength of liquefied soil in centrifuge models", *GeoCongress 2012*, ASCE, 1740-1749.

[5] Arulnathan, R., Boulanger, R.W., Kutter, B.L. and Sluis, W.K. (2000), "New tool for shear wave velocity measurements in model tests", *Geotechnical Testing Journal*, **23**(4), 444–453.

[6] Asgarian, B., Aghakouchak, A., Alanjari, P. and Assareh, M., (2008), "Incremental dynamic analysis of jacket type offshore platforms considering soil-pile interaction", *14th World Conf. on Earth. Eng.*, Beijing, China.

[7] Asgarian., B., Zarrin, M. and Boroumand, M. (2013) "Nonlinear dynamic analysis of pile foundation subjected to strong ground motion using fiber elements", *International Journal of Maritime Technology*, **1**(1):35-46.

[8] Asgarian, B., Zarrin, M. and Sabzeghabaian, M. (2018) "Effect of foundation behavior on steel jacket offshore platform failure modes under wave loading", *Ships and Offshore Structures*, In press. DOI: 10.1080/17445302.2018.1526862.

[9] Ashford, S.A., Boulanger, R.W. and Brandenberg, S.J. (2011), "Recommended Design Practice for Pile Foundations in Laterally Spreading Ground", *Peer Publication, PEER 2011/04*, Uni. Berk., Calif.

[10] Assareh, M.A. and Asgarian, B. (2008), "nonlinear behavior of single piles in jacket type offshore platforms using incremental dynamic analysis", *American Journal of Applied Sciences*, **5**(12), 1793-1803.

[11] Balakrishnan, A. (2000), "Liquefaction remediation at a bridge site", *Ph.D dissertation*, University of California, Davis, Calif.

[12] Bea, RG. (1991), "Earthquake geotechnology in offshore structures", *Proc. 2nd Int. Conf. on Recent Advances in Geotechnical Earthquake Eng. and Soil Dyn.*, No.SOA13, St. Louis, MI.

[13] Berger, E., Mahin, S.A. and Pyke, R. (1977), "Simplified method for evaluating soil–pile–structure interaction effects", *Proc. of 9th Offshore Technology Conference, OTC*, paper 2954, Huston, Texas, 589 – 598.

[14] Biot, M.A. (1962), "The mechanics of deformation and acoustic propagation in porous media" *J. Appl. Phys.*, **33**(4), 1482–1498.

[15] Boulanger, R.W., Curras, C.1., Kutter, B.L., Wilson, D.W. and Abghari, A. (1999), "Seismic soil-pile-structure interaction experiments and analyses", *Geotech. and Geoenvironmental Eng.*, ASCE, **125**(9), 750-759.

[16] Boulanger, R.W., Kutter, B.L., Brandenberg, S.J., Singh, P. and Chang, D. (2003), "Pile foundations in liquefied and laterally spreading ground during earthquakes: Centrifuge experiments and analyses", *Report UCD/CGM-03/01*, Center for Geotechnical Modeling, Univ. of California, Davis, CA, pp: 205.

[17] Brandenberg, S. (2005), "Behavior of pile foundations in liquefied and laterally spreading ground", *Ph.D thesis*, University of California, Davis, Calif.

[18] Byrne, P.M., Park, S.S., Beaty, M., Sharp, M., Gonzalez, L. and Abdoun, T. (2004), "Numerical modeling of liquefaction and comparison with centrifuge tests", *Canadian Geotech. J.*, **41**(2), 193-211.

[19] Chan, A.H.C. (1988), "A unified finite element solution to static and dynamic problems in geomehanics" *Ph.D dissertation*, Univ. College of Swansea, Swansea, U.K.

[20] Cooke, G. (2000), "Ground improvement for liquefaction mitigation at existing highway bridges", PhD. Thesis, Depart. of Civil and Envir. Engng., Virg. Polytec. Inst. and State University.

[21] De Souza, R. M. (2000), "Force-Based finite element for large displacement inelastic analysis of frames", *Ph.D Thesis*, Depart. of Civil and Envir. Engng., University of California, Berkeley.

[22] Elsayed, T., El-Shaib, M. and Gbr, K. (2014) "Reliability of fixed offshore jacket platform against earthquake collapse", Ships and Offshore Structure, **11**(2):167-181.

[23] Ganainy, H.E., Abdoun, T. and Dobry, R. (2012), "Centrifuge study of the effect of permeability and other soil properties on the liquefaction and lateral spreading of dense sand", *GeoCong. 2012*, ASCE, 1998-2007.

[24] Georgiadis, M. (1983), "Development of p-y curves for layered soils", *Proc. Conf. Geotech. Pract. Offshore Engng., Am. Soc. Civ. Engrs.* 536-545.

[25] Fredlund, D.G. and Rahardjo, H. (1993), "Soil mechanics for unsaturated soils", *A Wiley-Interscience Publication*, John Wiley L Sons, Inc.

[26] Hardin, B.O. and Drnevich, V.P. (1970), "Shear modulus and damping in soils-II: Design equations and curves", *Rep. No. UKY 27-70-CE3*, Soil Mechanics Series No. 2, 49, Univ. of Kentucky, Lexington, Ky.

[27] Holtz, R.D. and Kovacs, W.D. (1981), "An introduction to geotechnical engineering", Prentice Hall, Englewood Cliffs, New Jersey.

[28] Honarvar, M., Bahaari, M., Asgarian, B. and Alanjari, P. (2007), "Cyclic inelastic behavior and analytical modelling of pile–leg interaction in jacket type offshore platforms", *Applied Ocean Rese.*, **29**(4), 167–179.

[29] Idriss, I.M. and Boulanger, R.W. (2007), "SPT- and CPT-based relationships for the residual shear strength of liquefied soils", *Earthquake Geotechnical Engineering, Proc., 4th Intl. Conf. on Earthq. Geotech. Engrg*., Invited Lectures, K. D. Pitilakis, ed., Springer, The Netherlands, pp. 1-22.

[30] Imamura, S. (2010), "Characteristics of horizontal subgrade reaction of piles in liquefiable sand", *Physical Modelling in Geotechnics*, Taylor & Francis Group, 1403-1408, London.

[31] Ishihara, K. (1994), "Review of the predictions for Model 1 in the VELACS program",*Verification Of Numerical Procedures For The Analysis Of Soil Liquefaction Problems*. Rotterdam,1353–68.

[32] Kutter, B.L., Idriss, I.M., Khonke, T., Lakeland, J., Li, X-S., Sluis, W., Zeng, X., Tauscher, R.C., Goto, Y. and Kubodera I. (1994), ''Design of a large earthquake simulator at UC Davis'', *Proc. Conf. Centrifuge*, Rotterdam, The Netherlands, 169–175.

[33] Liu, L. and Dobry, R. (1995), "Effect of liquefaction on lateral response of piles by centrifuge model tests" *National Center for Earthquake Engineering Research (NCEER) Bulletin*, **9**(1), 7–11.

[34] Matlock, H. (1970), "Correlations for design of laterally loaded piles in soft clay", *Proc. 2nd Offshore Technology Conf.*, OTC 1204, Houston.

[35] Mazzoni, S., McKenna, F., Scott, M. and Fenves, G. (2007), "Open System for Earthquake Engineering Simulation (OpenSees)", *Command Language Manual*, University of California, Berkeley, 1th July.

[36] Nemat-Nasser, S., and Tobita, Y. (1982), ‘‘Influence of fabric on liquefaction and densification potential of cohesionless sand.’’ *Mech. Mater.*, **1**, 43– 62.
[37] O'Neill, M. and Murchison, J. (1983), "An evaluation of p-y relationships in sands", *Report GT-DF02-83*, Dept. of Civil Eng., Univ. of Houston, May.
[38] Park, S.S. and Byrne, P.M. (2004), "Stress densification and its evaluation", *Canad. Geotech. J.*, **41**(1), 181–186.
[39] Rollins, K., Gerber, T., Lane, J. and Ashford, S. (2005), "Lateral resistance of a full-scale pile group in liquefied sand", *Journal of Geotechnical and Geoenvironmental Engineering*, **131**(1), 115–125.
[40] Seed, H.B. and Idriss, I.M. (1970), "Soil moduli and damping factors for dynamic response analyses", *Report No. EERC 70-10*, *Earthquake Eng. Research Center*, University of California, Berkeley, Cali.
[41] Shahir, H., Pak, A., Taiebat, M. and Jeremic, B. (2012), "Evaluation of variation of permeability in liquefiable soil under earthquake loading ", *J. Computers and Geotechnics*, **40**, 74–88.
[42] Sharifian, H., Bargi, K. and Zarrin, M. (2015) "Ultimate Strength of Fixed Offshore Platforms Subjected to Near-Fault Earthquake Ground Vibration", Shock and Vibration, **2015**:1–19. Article ID 841870. DOI:10.1155/2015/841870
[43] Sze, H.Y. and Yang J. (2014), "Failure Modes of Sand in Undrained Cyclic Loading: Impact of Sample Preparation", *Geotech. and Geoenvironmental Eng.*, ASCE, **140**(1), 152-169.
[44] Taiebat, M., Shahir, H. and Pak, A. (2007), "Study of pore pressure variation during liquefaction using two constitutive models for sand", *Soil Dynam Earthq Eng*, **27**(1), 60–72.
[45] Tokimatsu, K., Suzuki, H. and Suzuki, Y. (2001), "Back-calculated p-y relation of liquefied soils from large shaking table tests", *4th Conf. on Recent Adv. in Geotech. Earthq. Eng. and Soil Dyn*. San Diego, Calif.
[46] Tokimatsu, K. and Suzuki, H. (2004), "Pore water pressure response around pile and its effects on p-y behavior during soil liquefaction", *Soils and Foundations*, **44**(6), 101–110.
[47] U.C., Davis website http://nees.ucdavis.edu.
[48] Vucetic, M. and Dobry, R. (1991), "Effect of soil plasticity on cyclic response", *Journal of Geotechnical Engineering*, ASCE, **117**(1), 89–107.
[49] Wang, S., Kutter, B.L., Chacko, J.M., Wilson, D.W., Boulanger, R.W. and Abghari, A. (1998), ‘‘Nonlinear seismic soil-pile-structure interaction.’’ *Earthquake Spectra*, **14**(2), 377–396.
[50] Weaver, T., Ashford, S. and Rollins, K. (2005), "Response of 0.6 m cast-in-steel-shell pile in liquefied soil under lateral loading", *Journal of Geotechnical and Geoenvironmental Engineering*, **131**(1), 94–102.
[51] Wilson, D.W., Boulanger, R.W. and Kutter, B.L. (1997a), ‘‘Soil-pile superstructure interaction at soft or liquefiable soil sites—Centrifuge data report for Csp4’’, *Rep. No. UCD/CGMDR-97/05*, Ctr. for Geotech. Modeling, Dept. of Civ. and Envir. Engrg., University of California, Davis, Calif.
[52] Wilson, D.W., Boulanger, R.W. and Kutter, B.L. (1997b), ‘‘Soil-pile superstructure interaction at soft or liquefiable soil sites—Centrifuge data report for Csp5.’’ *Rep. No. UCD/CGMDR-97/06*, Ctr. for Geotech. Modeling, Dept. of Civ. and Envir. Engrg., University of California, Davis, Calif.
[53] Wilson, D.W. (1998), ‘‘Soil-pile-superstructure interaction in soft clay and liquefiable sand’’ *Rep. No. UCD/CGM-98/04*, Ctr. for Geotech. Modeling, Dept. of Civ. and Envir. Engrg., Uni. of California, Davis, Calif.
[54] Wilson, D.W., Boulanger, R.W. and Kutter, B.L. (2000), "Observed seismic lateral resistance of liquefying sand", *Jour. of Geotechnical and Geoenvironmental Eng.*, ASCE, **126**(10), 898-906.
[55] Yang, Z. (2000), ‘‘Numerical modeling of earthquake site response in-cluding dilation and liquefaction.’’ *Ph.D dissertation*, Dept. of Civil Engineering and Engineering Mechanics, Columbia University, New York.
[56] Yang, Z. and Elgamal, A. (2002), "Influence of permeability on liquefaction-induced shear deformation", *J Eng Mech*, **128**(7), 720–9.
[57] Yang, Z., Elgamal, A. and Parra, E. (2003), "Computational model for cyclic mobility and associated shear deformation", *Journal of Geotechnical and Geoenvironmental Engineering*, ASCE, **129**(12), 1119–1127.
[58] Youd, T.L. and Idriss, I.M. (1997), "Proceeding of the NCEER Workshop on Evaluation of Liquefaction Resistance of Soils", National Cent. For Earthq. Eng. Res., State Uni. Of New York at Buffalo.
[59] Zarrin, M., Asgarian, B. and Abyani, M. (2018) "Probabilistic seismic collapse analysis of jacket offshore platforms", *ASME Journal of Offshore Mechanic and Arctic Engineering*, **140**(3):031601.
[60] Zarrin, M. and Asgarian, B. (2013) "Reducing Error of Probabilistic Seismic Demand Analysis of Jacket Type Offshore Platforms Subjected to Pulse-Like Near Fault Ground Motions", *Journal Of Marine Engineering*, **8** (16):33-49
[61] Zeng, X. and Liu, G. (2012), "Liquefaction of Dense Sand under Earthquake Loading", *GeoCongress 2012*, ASCE, 1670-1679.